Supplementary data

Different toxicity of nanoscale titanium dioxide particle in the roots and leaves of wheat seedling

Yanger Chen,*‡[a] Nan Wu,‡[a] Haotian Mao,‡[a] Jun Zhou,[a] Yanqiu Su,[c] Zhongwei Zhang,[b] Huaiyu Zhang,[a] and Shu Yuan[b]

[a] *College of Life Science, Sichuan Agricultural University, Ya'an 625014, China. E-mail: anty9826@163.com; Tel: +86-835-2886653*

[b] *College of Resources, Sichuan Agricultural University, Chengdu 611130, China*

[c] *College of Life Science, Sichuan University, Chengdu 610064, China*

‡ These authors contributed equally to this work.

Supplementary data contents

Supplemental Methods

Measurements of chlorophyll, proline, soluble sugar, and total protein

Chlorophyll contents from fresh wheat leaves were measured by a 80% (v/v) acetone extraction method at 646 and 663 nm absorbance.[1] Soluble sugar and proline were extracted from fresh wheat leaves and roots (0.5 g) using an 80% ethanol solution. Soluble sugar was colorimetrically quantified after reacting with anthrone reagent according to the previous method using a UV spectrophotometer (Hitachi-U2000, Hitachi, Ltd., Tokyo, Japan).[2] Proline content in roots and leaves was determined by measuring the absorbance at 520 nm using a UV spectrophotometer according to the previous method.[3] The total proteins was determined as described previously using a UV spectrophotometer.[4]

Measurements of ROS and cell death

Visualization of hydrogen peroxide (H_2O_2) and superoxide ($O_2^{\cdot-}$) in the leaves and roots was performed by 2 g mL^{-1} 3,3-diaminobenzidine (DAB) solution for 10 h and 0.5 g mL^{-1} nitro blue tetrazolium (NBT) solution for 2 h, respectively. Stained roots and leaves were washed in 95% ethanol at 80°C until other color was nearly removed.[5] For quantitative analysis of ROS, the content of $O_2^{\cdot-}$ and H_2O_2 in wheat roots and leaves was determined according to the method of Elstner and Heupel and Okuda et al., respectively.[6,7] To visualize the degree of cell death, wheat roots and leaves after *n*TiO_2 exposure were submerged in 1.25 mg/mL trypan-blue solution and then decolorized in chloral hydrate solution as following the method of Shirasu et al.[8]

Measurements of lipid peroxidation and electrolyte leakage

Malonyldialdehyde (MDA) level in wheat roots and leaves was measured using a UV spectrophotometer following the previous method.[9] Lipid peroxidation was expressed as thiobarbituric reactive species (TBARS) (extinction coefficient of 155 mM^{-1} cm^{-1}). Electrolyte leakage was measured with a conductivity meter (DDSJ-308A, Shanghai Precision Instruments Co., Ltd., China) according to the method of Chen et al.[9] The relative electrolyte leakage was calculated as the ratio of the initial conductivity to the absolute conductivity (boiled at 95°C for 30 min).

Measurements of antioxidant enzyme and non-enzymatic antioxidants

The crude extracts for antioxidant enzymes from the roots and leaves were conducted according to the previous method.[10] The treated roots and leaves were ground with ice-cold 50 mM potassium phosphate buffer (pH 7.8) including 0.2m M EDTA, 2% (w/v) polyvinyl polypyrrolidone (PPVP) and 2 mM ascorbate. After centrifugation (15 min, 12,000 g), the supernatant was applied for measurements of enzyme activity. Catalase (CAT), peroxidase (POD), superoxide dismutase (SOD), ascorbate peroxidase (APX), glutathione peroxidase (GPX), and glutathione reductase (GR) activities were assayed as previously described.[10] The assays were performed using a UV spectrophotometer (Hitachi-U2000, Hitachi, Ltd., Tokyo, Japan).

Contents of reduced ascorbic acid/dehydroascorbate (AsA/DHA) were analyzed in extracts

according to the method of Kampfenkel et al.[11] The measurement is based on the reduction of Fe^{3+} to Fe^{2+} by AsA. Then, Fe^{2+} forms complexes with bipyridyl giving a pink color that absorbs at 525 nm. The contents of AsA and AsA+DHA were calculated using l-ascorbate as the standard. DHA content was determined using total ascorbate minus AsA. Reduced glutathione/oxidized glutathione (GSH/GSSG) contents were determined following the method of Griffith.[12]

Gas exchange measurements

Net photosynthetic rate (*P*n), stomatal conductance, transpiration rate, and intercellular CO_2 concentration were measured using the GSF-3000 photosynthesis system (Heinz-Walz Instruments, Effeltrich, Germany) under 360 μmol mol^{-1} CO_2 concentration and illumination of 1,500 μmol photon m^{-2} s^{-1} at room temperature according to the previous method.[5] Gas exchange parameters were calculated as described previously.[13]

Supplemental Table 1

Table S1 Seeding growth, germination rate, and the contents of total chlorophyll and proteins in wheat germinated and grown in $n\text{TiO}_2$ suspension for 14 days.

$n\text{TiO}_2$ Concentration (g L^{-1})	Root Length (cm)	Seeding Length (cm)	Germination rate (%)	Total Chlorophyll (mg g^{-1} FW)	Chlorophyll *a/b*	Total Protein (mg g^{-1} FW)
0	11.92 ± 1.85a	13.81 ± 1.32a	97.12 ± 5.31a	2.53 ± 0.13a	3.28 ± 0.15a	8.53 ± 0.31a
0.1	10.98 ± 2.21ab	12.62 ± 1.95ab	95.43 ± 4.17a	2.04 ± 0.09ab	3.12 ± 0.11ab	8.04 ± 0.43a
0.5	10.23 ± 1.56ab	12.05 ± 1.48ab	94.52 ± 3.85a	1.95 ± 0.09b	3.05 ± 0.07b	8.12 ± 0.44a
1.0	9.54 ± 1.32b	11.23 ± 1.63b	82.29 ± 4.23b	1.95 ± 0.12b	2.87 ± 0.10bc	7.86 ± 0.35ab
5.0	7.43 ±1.69c	8.56 ± 1.69c	71.43 ± 3.75c	1.81 ± 0.09c	2.76 ± 0.015c	7.55 ± 0.31b

Values are means ± SD from four independent biological replicates. Different letters show a significant difference among these treatments following Duncan's multiplication range test when $P < 0.05$.

Supplemental Figures 1-10

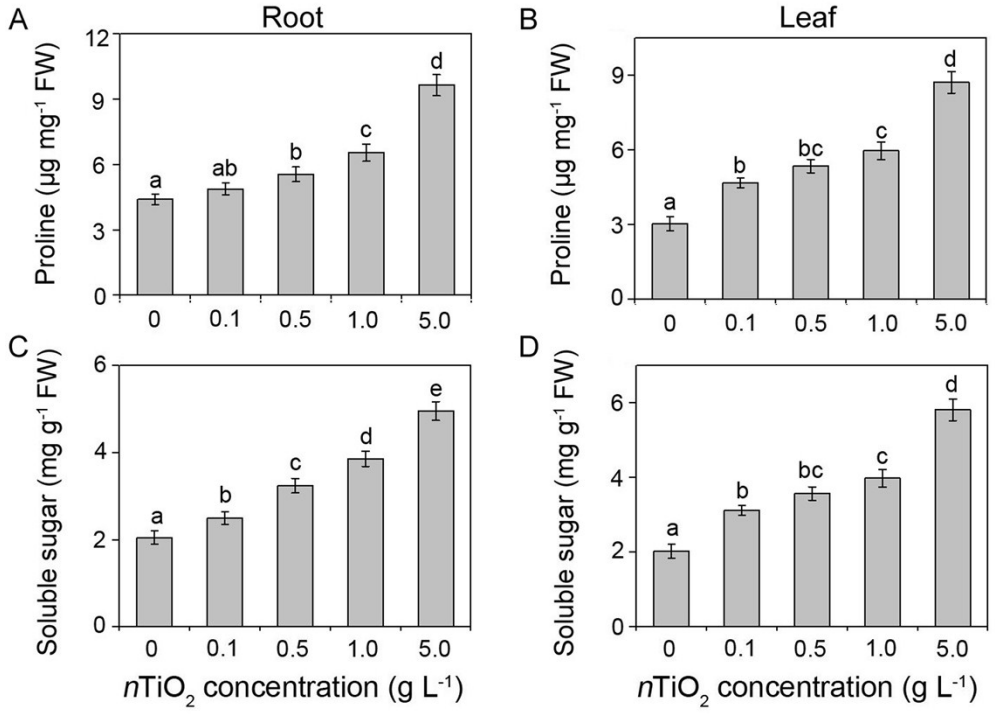

Fig. S1 Osmotic regulators in the roots (A and C) and leaves (B and D) of CN19 under $n\text{TiO}_2$ exposure for 14 days. The data are represented as mean ± SD from four independent repetitions (n = 4). The Duncan's multiple range test showed that the values corresponding to the different letters were significantly different at $P < 0.05$.

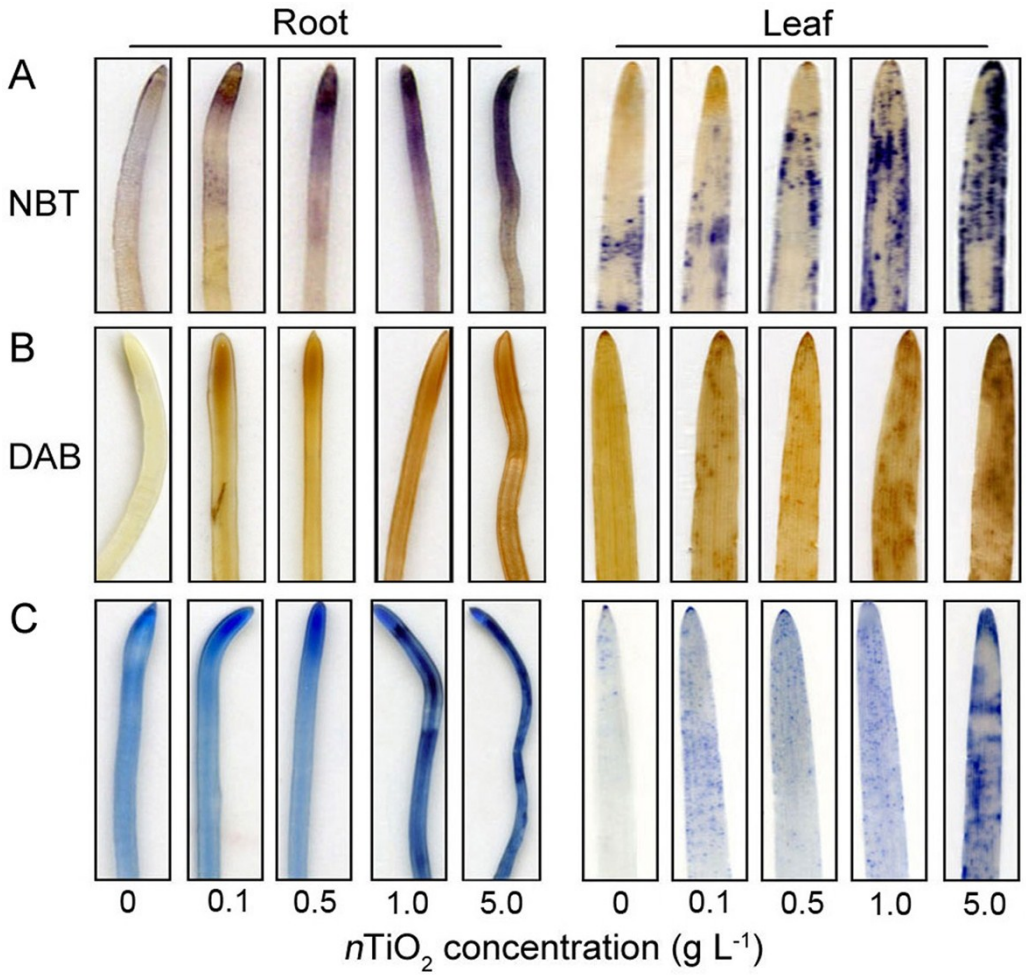

Fig. S2 Histochemical assays of ROS and cell death in CN19 under $n\text{TiO}_2$ exposure for 14 days. The staining of $O_2^{\cdot-}$ and H_2O_2 was done by nitro blue tetrazolium (NBT) (A) and 3,3-diaminobenzidine (DAB) (B) in the roots and leaves, respectively. Microscopic cell death was observed in the roots and leaves by trypan blue staining (C).

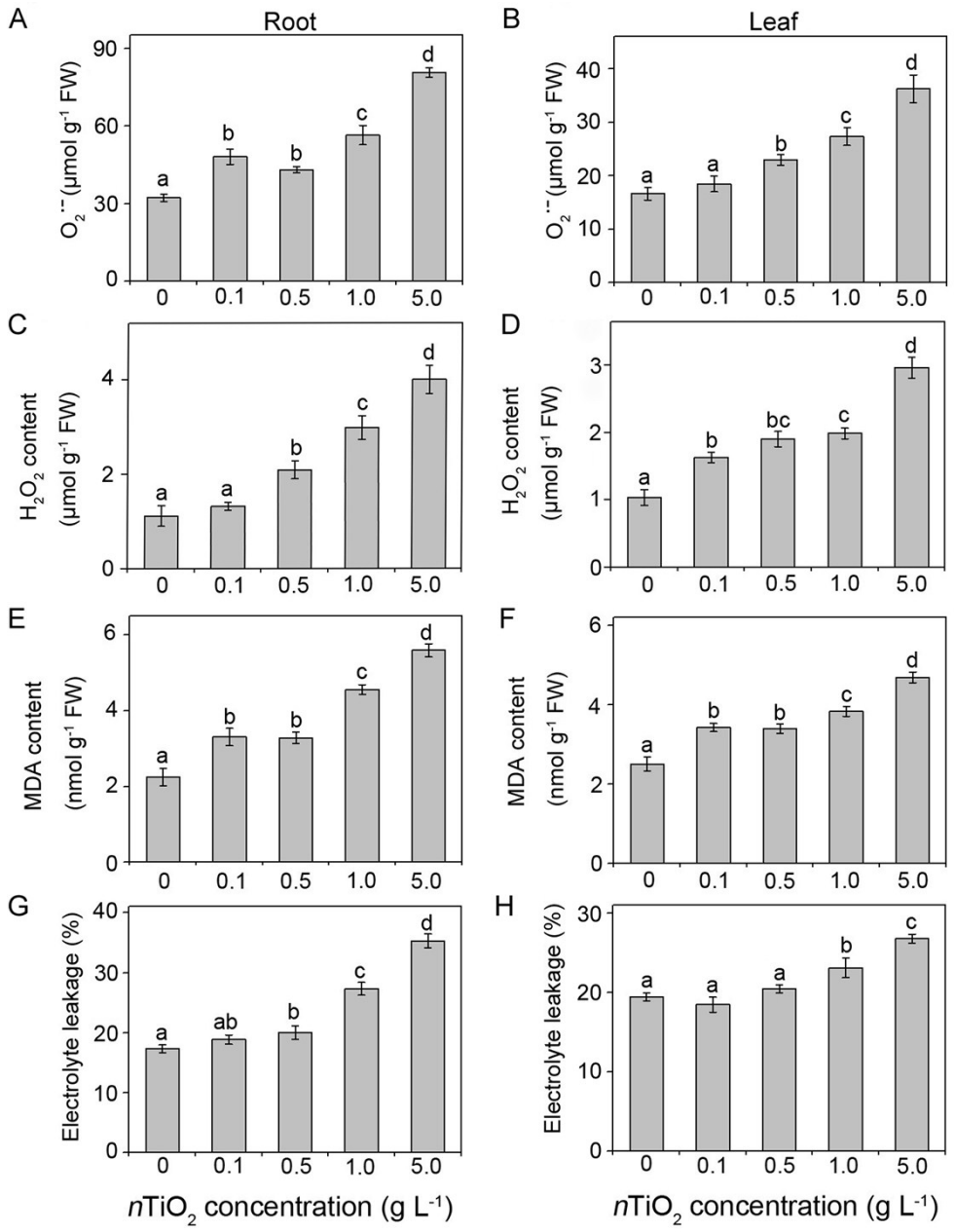

117

118 **Fig. S3** ROS accumulation (A-D) and lipid peroxidation (E-H) in the roots and leaves of

119 CN19 under nTiO$_2$ exposure for 14 days. The data are represented as mean ± SD for four

120 independent repetitions (n = 4). The Duncan's multiple range test showed that the values

121 corresponding to the different letters were significantly different at $P < 0.05$.

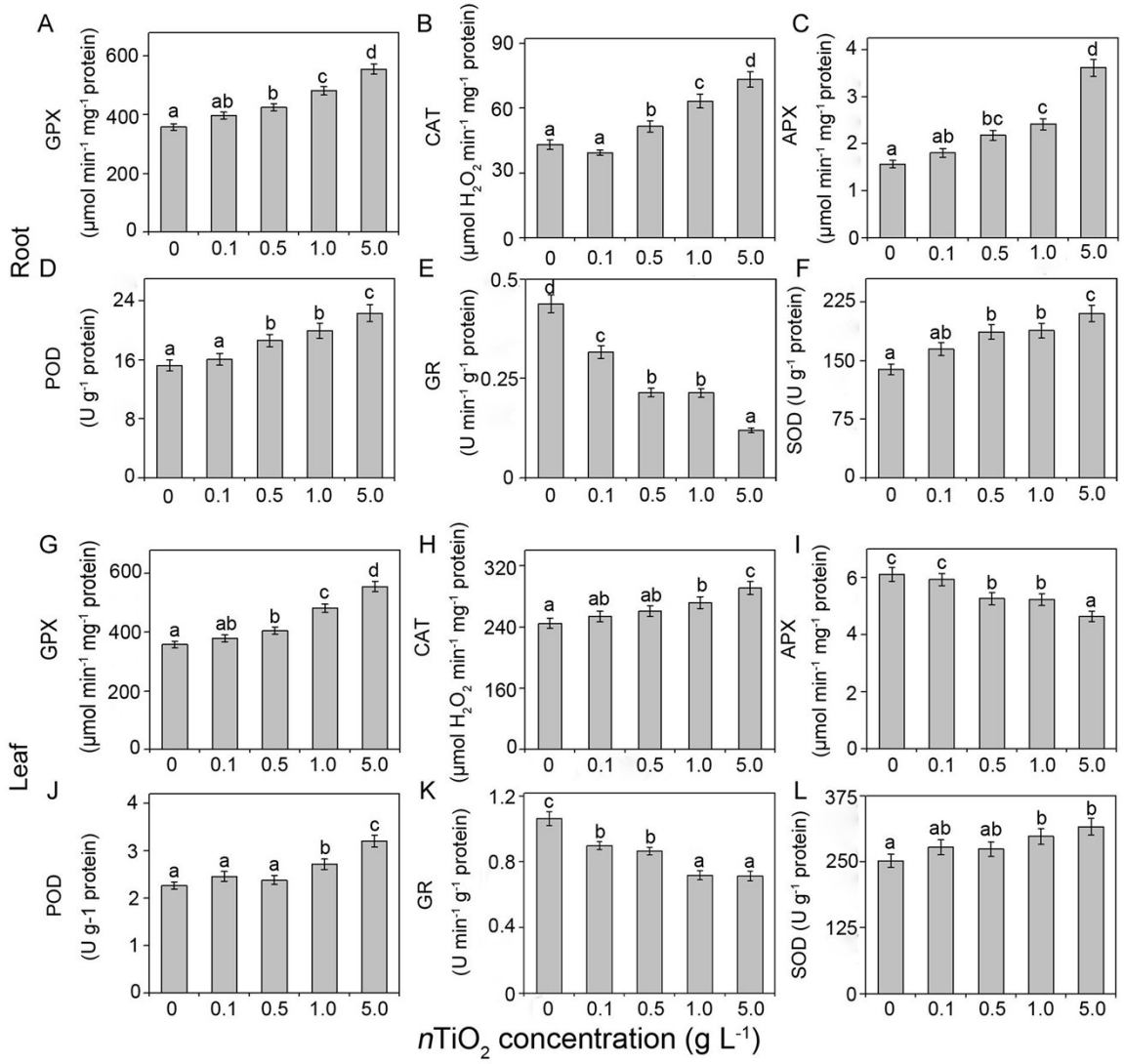

122

123 **Fig. S4** The activities of antioxidant enzymes in the roots (A-F) and leaves (G-L) of CN19

124 under $n\text{TiO}_2$ exposure for 14 days. POD, peroxidase; SOD, superoxide dismutase; catalase

125 CAT, catalase; APX, ascorbate peroxidase; GPX, glutathione peroxidase; and GR,

126 glutathione reductase. The data are represented as mean ± SD for four independent repetitions

127 (n = 4). The Duncan'smultiple range test showed that the values corresponding to the

128 different letters were significantly different at $P < 0.05$.

129

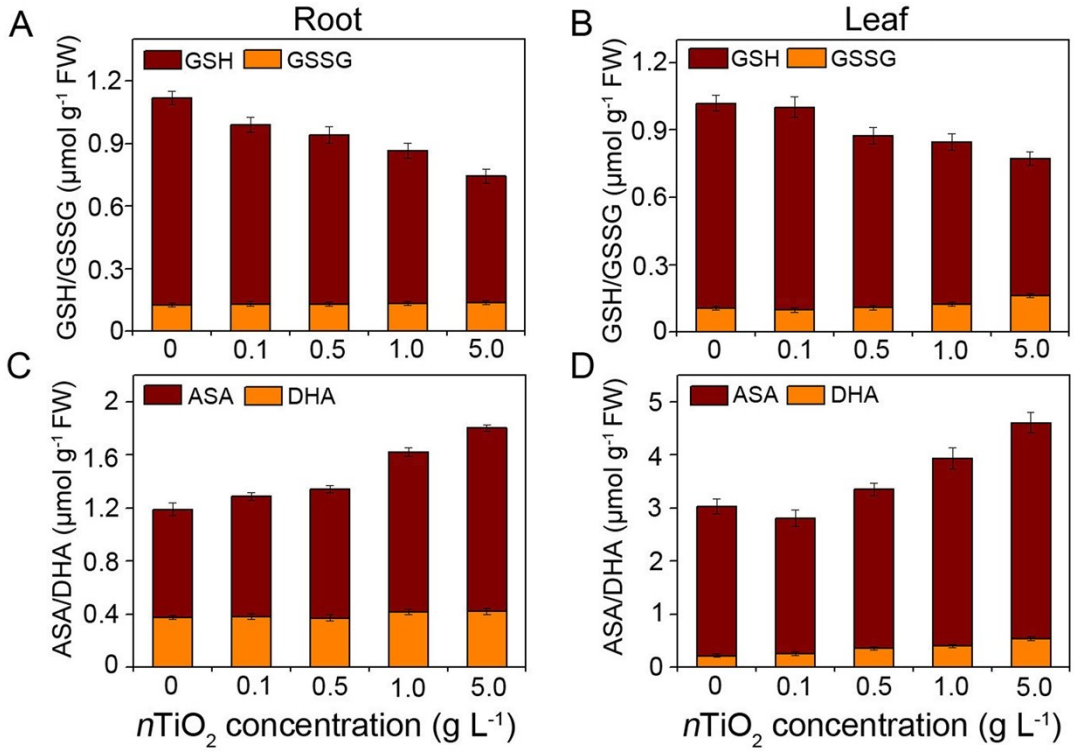

Fig. S5 The content of non-enzyme antioxidant in the roots and leaves of CN19 under $n\mathrm{TiO_2}$ exposure for 14 days. AsA and DHA (A and C), reduced ascorbic acid and dehydroascorbate, respectively; GSH and GSSG (B and D), reduced and oxidized glutathione, respectively. Data is presented as mean ± SD for four replicates. Values with a common letter are statistically different at $P < 0.05$ according to Duncan's multiple range test.

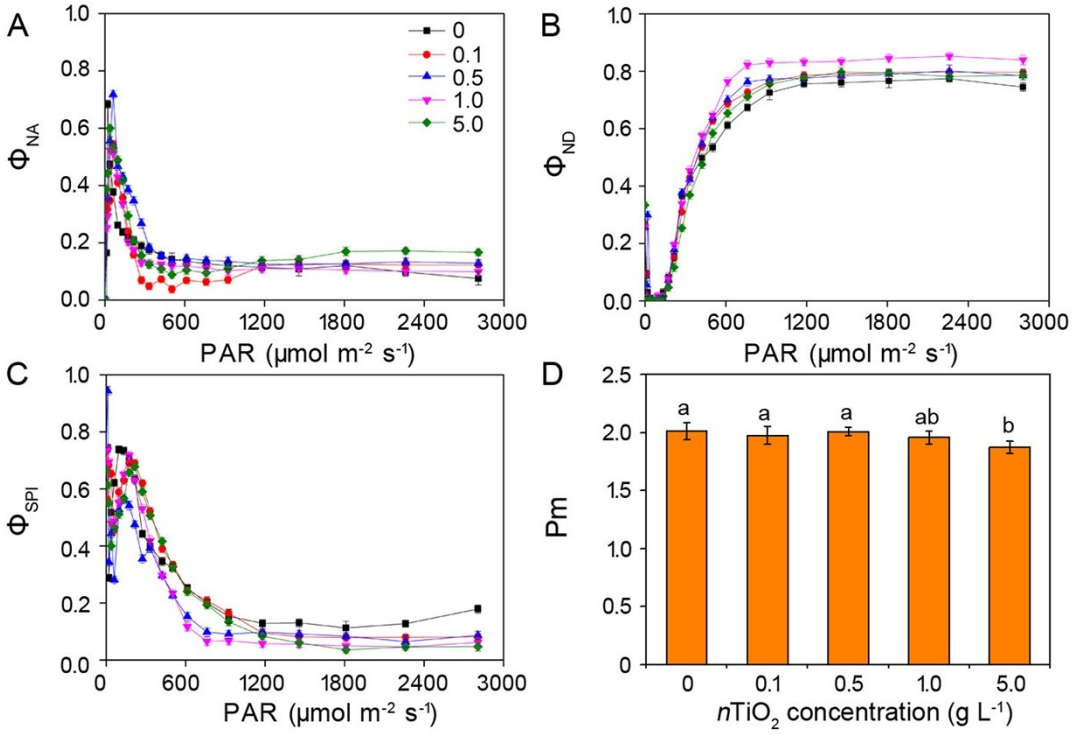

Fig. S6 Parameters derived from P700 absorbance in CN19 under *n*TiO_2 exposure for 14 days. Φ_{NA} (A), acceptor side limitation of quantum yield at the PSI reaction center for non-photochemical energy dissipation; Φ_{ND} (B), honor side limitation of quantum yield at the PSI reaction center for non-photochemical energy dissipation; ΦPSI (C), effective quantum yield of PSI; Pm (D), maximal P700 signal. Data is presented as mean ± SD for four replicates. Values with a common letter are statistically different at $P < 0.05$ according to Duncan's multiple range test.

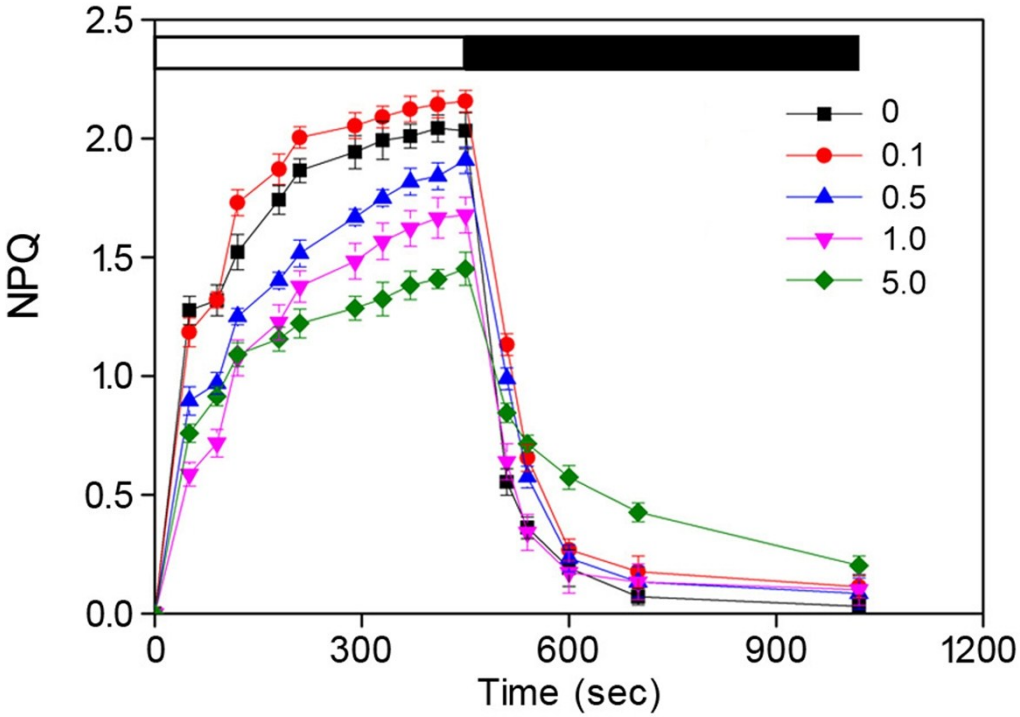

Fig. S7 None-photochemical quenching (NPQ) kinetics of CN19 under *n*TiO_2 exposure for 14 days. Wheat seedlings illuminated with 1000 µmol photons m^{-2} s^{-1} for 10 min with a 15 min period darkness, as indicated by the white and black bars. Data is represented as mean ± SD for four replicates.

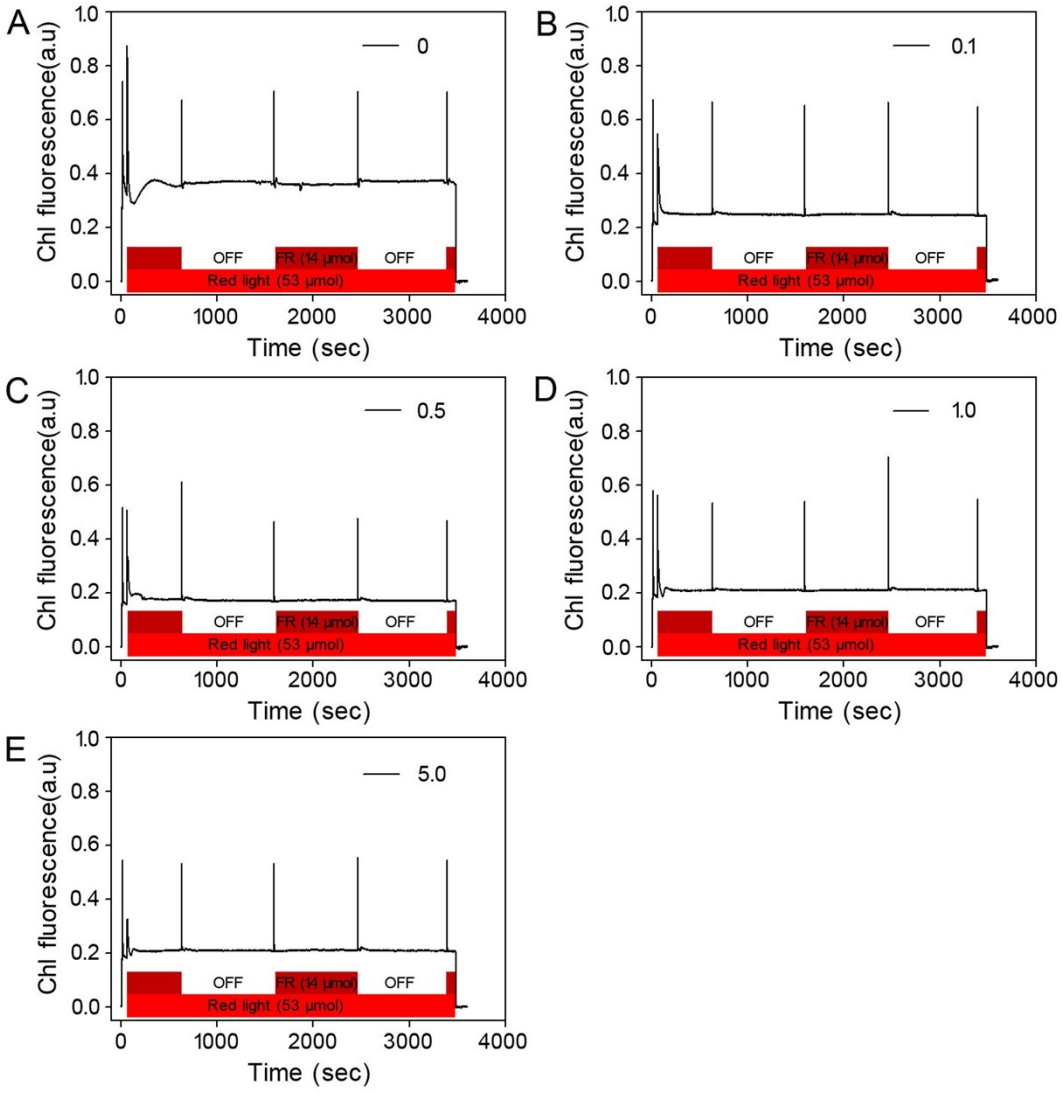

166

167 **Fig. S8** Assays of state transitions of CN19 under *n*TiO_2 exposure for 14 days. Pulse

168 amplitude-modulated fluorescence traces after shifts from state 1 to state 2 light and back for

169 different treatments. The bars at the bottom indicate illumination with red (shown in red) and

170 far-red (dark red) light. Fluorescence is shown in arbitrary units.

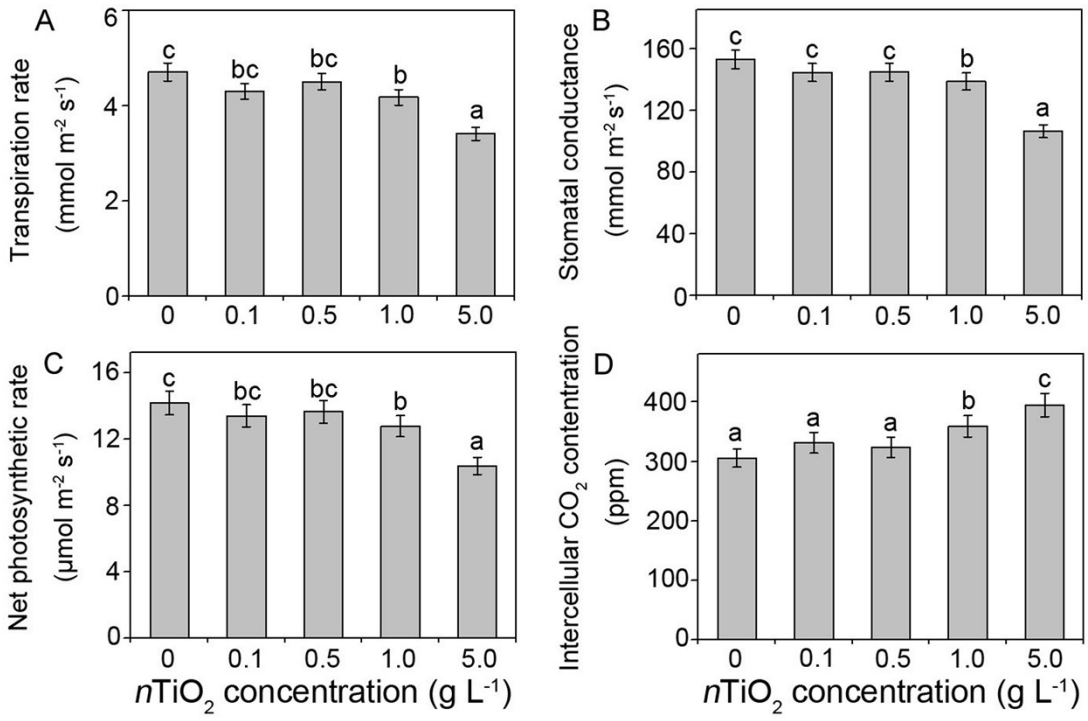

171

172 **Fig. S9** Transpiration rate (A), stomatal conductance (B), net photosynthetic rate (C),

173 intercellular CO_2 concentration (D) of CN19 under nTiO$_2$ exposure for 14 days. Data is

174 presented as mean ± SD for four replicates. Values with a common letter are statistically

175 different at $P < 0.05$ according to Duncan's multiple range test.

176

177

178

179

180

181

182

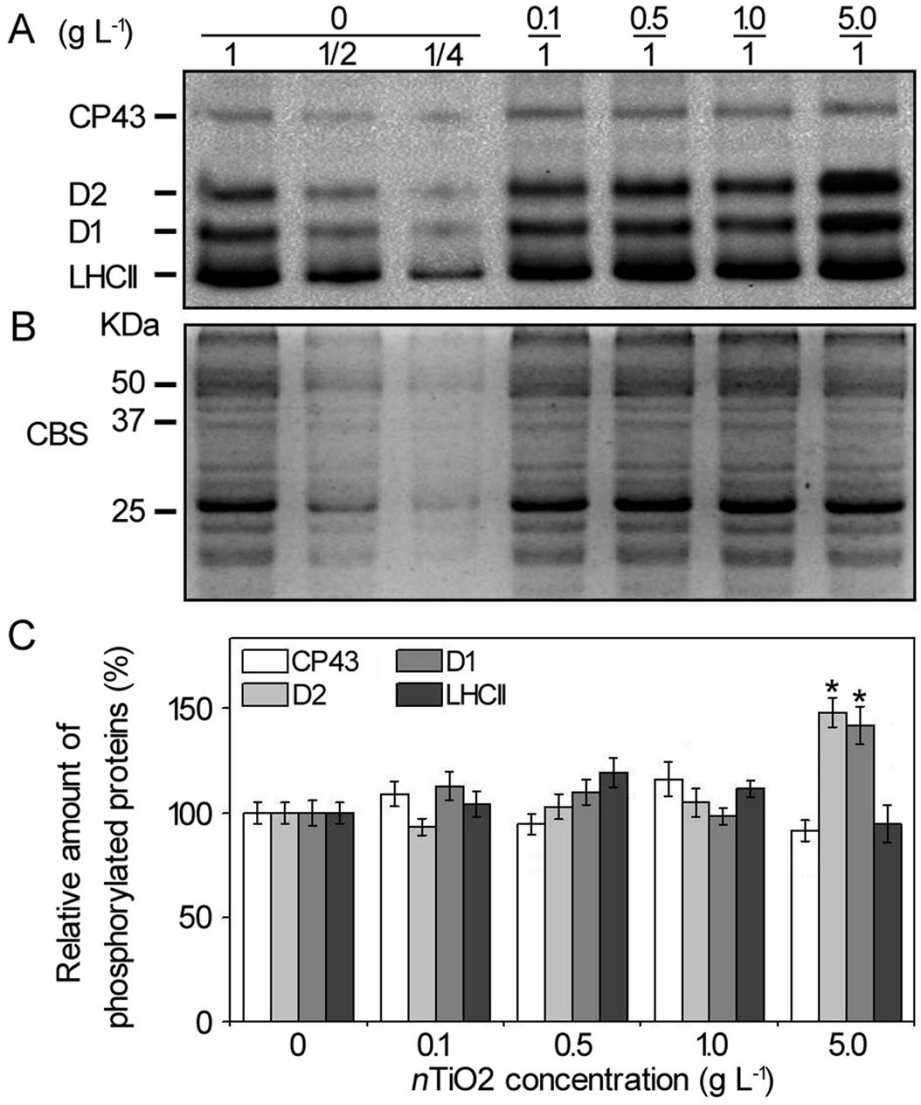

183

184 **Fig. S10** PSII protein phosphorylation of CN19 under $n\text{TiO}_2$ exposure for 14 days. (A)
185 Immunoblot analyses of thylakoid membrane proteins were conducted using anti-
186 phosphothreonine antibodies. An equal amount of total Chl (1 μg of Chl) was loaded into each
187 well. (B) Coomassie blue staining (CBS) of SDS-PAGE were showed. Loading was done
188 based on equal amount of total Chl (1 μg). (C) Quantitative analysis of immunoblot data. The
189 results are given relative to the content of control (100%). The significant differences were
190 marked with asterisks when $P < 0.05$ ($n = 4$).

191

Supplemental References

1 R. J. Porra, W. A. Thompson, and P. E. Kriedemann, *Biochim. Biophys. Acta*, 1989, **975**, 384–394.

2 J. Thomas, *Percept. Psychophys*, 1977, **22**, 310–312.

3 L. S. Bates, R. P. Waldren, and I. D. Teare, *Plant Soil*, 1973, **39**, 205–207.

4 O. H. Lowry, N. J. Rosebrough, A. L. Farr and R. J. Randall, *J. Biol. Chem.*, 1951, **193**, 265–275.

5 Y. E. Chen, J. Ma, N. Wu, Y. Q. Su, Z. W. Zhang, M. Yuan, H. Y. Zhang, X. Y. Zeng and S. Yuan, *Plant Physiol. Biochem.*, 2018, **130**, 267–276.

6 E. F. Elstner and A. Heupel, *Anal. Biochem.*, 1976, **70**, 616–620.

7 S. I. Okuda, K. Ito, H. Ozawa and K. Izaki, *J. Ferment. Bioeng.*, 1991, **71**, 424–429.

8 K. Shirasu, T. Lahaye, M. W. Tan, F. Zhou, C. Azevedo and P. Schulze-Lefert, *Cell*, 1999, **99**, 355–366.

9 Y. E. Chen, C. M. Zhang, Y. Q. Su, J. Ma, Z. W. Zhang, M. Yuan, H. Y. Zhang and S. Yuan, *Environ. Exp. Bot.*, 2017, **135**, 45–55.

10 J. Xu, Y. Y. Zhu, Q. Ge, Y. L. Li, J. H. Sun, Y. Zhang and X. J. Liu, *New Phytol.*, 2012, **196**, 125–138.

11 K. Kampfenkel, S. Kushnir, E. Babiychuk, D. Inze and M. Van Montagu, *J. Biol. Chem.*, 1995, **270**, 28479–28486.

12 O. W. Griffith, *Anal. Biochem.*, 1980, **106**, 207–212.

13 S. Von Caemmerer and G. D. Farquhar, *Planta*, 1981, **153**, 376–387.